International Journal of Scientific Research & Engineering Trends
Volume 12, Issue 6, Nov-Dec-2026, ISSN (Online): 2395-566X

Finite Element-Based Wear Analysis of Automotive Disc Brake Pads Using Archard's Law: A Comparative Study of Friction Lining Materials

Shivani Baban Suryawanshi[1], Guide Dr. T Y Badgujar[2]
Department of Mechanical Engineering,
Late G N Sapkal College of Engineering, Anjneri, Nashik, Maharashtra, India[1,2]

Abstract — Disc brake performance and service life are strongly influenced by the tribological interaction between the brake pad and rotating rotor. Non-uniform contact pressure, frictional traction, material stiffness, and wear resistance can produce localised material removal and alter the contact state during repeated braking. This paper presents a finite-element-based framework for evaluating pad–rotor contact and predicting progressive wear using a generalised Archard wear formulation. The study is based on a three-dimensional modular brake-corner model described in the supplied project report. A 2.5 kN normal actuation load is considered, and tangential friction is represented through Coulomb friction. Three friction-lining candidates—organic composite, semi-metallic lining, and ceramic matrix composite—are compared using the reported elastic properties, friction coefficients, and dimensional wear coefficients. The source-reported numerical results indicate that inclusion of tangential traction changes the pressure field from a near-symmetric distribution to an asymmetric leading-edge concentration. Under the combined sliding-friction case, the organic baseline reaches approximately 15 µm maximum pad wear after about 2900 rotor revolutions (approximately 2.5 km sliding distance). Across the material cases, reported maximum wear depths are 15.0, 6.2, and 2.1 µm for organic, semi-metallic, and ceramic linings, respectively. The results demonstrate a trade-off between compliance, running-in duration, pressure concentration, and wear resistance. Since the numerical values are taken from the supplied report and were not independently rerun for this paper, they should be interpreted as reported simulation outputs requiring reproducibility and experimental validation.

Keywords— Disc brake, brake pad wear, finite element analysis, Archard's wear law, contact pressure, frictional contact, running-in, material comparison.

I. INTRODUCTION

Automotive braking systems convert vehicle kinetic energy into heat through friction between stationary pads and a rotating disc. Disc brakes are widely used because of their braking consistency, heat-dissipation capability, and relatively simple construction. During operation, the brake pads are clamped against the rotor by a caliper, producing a normal contact load and a tangential friction force. The resulting contact pressure and sliding motion govern the local frictional response and contribute to material loss.

Wear is not necessarily uniform across the pad surface. Geometric mismatch, component compliance, caliper support conditions, frictional traction, and thermal deformation can redistribute the contact load. High-pressure regions generally experience greater wear under a simple Archard-type model, although pressure alone does not determine the real wear rate. Sliding distance, material hardness or calibrated wear coefficient, temperature, velocity, and third-body effects can also be important.

Finite element analysis (FEA) offers a means of resolving the contact-pressure field and structural response of a brake assembly. When coupled to a wear update procedure, FEA can estimate the evolution of surface geometry and the redistribution of contact pressure during running-in. This paper consolidates the supplied project report into an IEEE-style research article and focuses on the reported comparison of three friction-lining material candidates.

The principal contributions are: (1) formulation of an FEA-to-wear workflow based on nodal contact pressure and sliding distance; (2) comparison of normal-only and combined normal/tangential loading; and (3) comparison of organic, semi-metallic, and ceramic lining candidates using reported wear and running-in metrics.

II. RELATED WORK

Prior disc-brake research has examined contact pressure, thermoelastic response, wear prediction, material selection, and brake noise. Archard's classical relation provides a compact

© 2026 IJSRET

link between normal pressure and sliding distance, while finite-element contact models resolve the non-uniformity of the pad–rotor interface [14]. Abu Bakar and Ouyang demonstrated the importance of suitable three-dimensional contact modelling for predicting disc-brake pressure distributions [13]. Ouyang et al. further coupled contact pressure with heat conduction and transient vibration, showing that thermal and mechanical effects are interdependent [15].

Wear-prediction studies have progressively incorporated experimentally characterised friction and wear behaviour. Riva et al. used finite-element methods to simulate brake wear and airborne particle emissions [8], while Gurumoorthy et al. evaluated finite-element wear prediction against laboratory and dynamometer data [3]. Grześ et al. highlighted the need to consider friction, temperature, braking time, and wear together when selecting lining materials [7]. Han et al. investigated thermo-mechanical analysis and pad-shape optimisation to reduce uneven wear [11]. Recent reviews and multiphysics studies continue to emphasise the dependence of brake wear on operating conditions and the need for calibrated model parameters [1], [2].

The supplied report identifies a practical gap in connecting a modular three-dimensional contact model with an iterative wear calculation and a comparative material assessment. The present paper addresses that project-level gap while retaining the source report's stated modelling assumptions and reported numerical values.

III. RESEARCH OBJECTIVES AND SCOPE

The study is organised around four objectives: (i) represent a passenger-car disc-brake pad–rotor subsystem in three dimensions; (ii) evaluate contact pressure under a defined normal load and frictional sliding condition; (iii) estimate progressive pad wear using Archard's law; and (iv) compare the predicted response of three candidate friction-lining materials. The reported analysis is primarily structural and isothermal. It does not establish a fully coupled transient thermal solution or experimentally measured service life. The paper therefore treats the numerical results as model-based predictions rather than direct evidence of field durability.

IV. NUMERICAL METHODOLOGY

1. Brake-Corner Model and Modular Decomposition

The project report describes a modular front brake-corner subsystem comprising a ventilated disc rotor, two friction pads (piston-side and finger-side), a floating single-piston caliper, a wheel-bearing/knuckle support arrangement, and simplified interfaces. For the wear-focused model, the principal bodies are the rotor, friction lining, backing plate, and piston representation. This decomposition reduces computational complexity while retaining the load path from piston actuation to the pad–rotor interface.

The CAD geometry is intended to represent the friction tracks and pad curvature. Small geometric details may be suppressed when they do not materially affect the contact region; however, any simplification can influence local stiffness and pressure distribution and should be recorded in a reproducible model definition.

2. Finite Element Discretisation and Contact

According to the supplied report, the steel backing plate and composite friction lining are represented using eight-node three-dimensional solid elements (SOLID185) with a characteristic element size of 3 mm. The hydraulic piston and grey cast-iron rotor are represented as rigid target surfaces (TARGE170) linked to pilot nodes. Pad-to-rotor interaction is defined as asymmetric surface-to-surface frictional contact using CONTA173/TARGE170 with an augmented-Lagrangian formulation. The backing-plate-to-lining interface is bonded, while the piston-to-backing-plate interface permits sliding and separation.

The piston pilot node is constrained in its transverse translations while axial actuation is permitted. A normal force of 2.5 kN is applied. Rotor rotation is prescribed through its pilot node. The report associates the actuation force with an equivalent hydraulic line pressure of approximately 1 MPa. This equivalence depends on the assumed piston area and should be checked against the actual model geometry before replication.

3. Frictional Loading

Tangential friction is represented using Coulomb's law:

$$F_f = \mu F_N \qquad (1)$$

where F_f is the tangential friction force, μ is the coefficient of friction, and F_N is the applied normal force. For the organic baseline ($\mu = 0.45$) and $F_N = 2.5$ kN, the nominal tangential force is 1.125 kN. The corresponding forces for the semi-metallic and ceramic candidates are 0.950 kN and 1.050 kN, respectively. The offset between the normal and tangential force paths produces a tipping moment that can shift the pressure field toward the leading side of the pad.

© 2026 IJSRET

4. Archard Wear Formulation

The project uses a dimensional form of Archard's wear law expressed as wear depth per unit sliding distance:

$$dh/ds = k\,p \qquad (2)$$

where h is superficial wear depth, s is sliding distance, p is local contact pressure, and k is a dimensional wear coefficient with units Pa^{-1}. For a node i at effective radius r_i, the sliding distance accumulated over n_j rotor revolutions is:

$$\Delta s_{i,j} = n_j\, 2\pi r_i \qquad (3)$$

An explicit Euler update is then applied:

$$h_{i,j} = h_{i,j-1} + k\, p_{i,j}\, \Delta s_{i,j} \qquad (4)$$

The reported APDL loop calculates contact pressure, evaluates nodal wear increments, updates the lining surface inward, and repositions rigid boundaries to close contact gaps before the next equilibrium solution. The formulation assumes the selected k remains constant during the simulated interval. A more general model would allow k to depend on temperature, pressure, sliding velocity, and material state.

5. Material Cases

Three friction-lining candidates are compared. Their properties, as stated in the source report, are summarised in Table I. These values are model inputs, not universal material constants; in particular, wear coefficients should be calibrated for the specific formulation and test conditions.

Table 1. Friction-Lining Material Inputs Reported in the Source Study

Material	E (GPa)	ν	k (Pa^{-1})	μ
Organic composite	10.0	0.10	1.00×10^{-14}	0.45
Semi-metallic lining	22.0	0.22	0.45×10^{-14}	0.38
Ceramic matrix composite	35.0	0.18	0.15×10^{-14}	0.42

The elastic modulus increases from 10 to 35 GPa across the candidates. The ceramic candidate is therefore the stiffest and is expected to conform less readily to the rotor. The wear coefficient decreases from 1.00×10^{-14} Pa^{-1} for the organic baseline to 0.15×10^{-14} Pa^{-1} for the ceramic candidate, indicating lower predicted wear for equal pressure and sliding distance under (2).

V. RESULTS AND DISCUSSION

1. Effect of Tangential Friction on Contact Pressure

The source report states that the normal-only case produces a near-symmetric pressure field, with a peak of approximately 1.2 MPa beneath the piston rim and low or zero contact toward portions of the pad edges. When rotor rotation and friction are introduced, tangential traction generates a tipping moment. The reported result is an asymmetric pressure field with increased pressure toward the leading edge and unloading or separation toward the trailing edge.

This comparison indicates that a normal-force-only model may not capture the pressure asymmetry associated with sliding friction. Since the wear increment in (4) is proportional to local pressure, the asymmetric case also produces a non-uniform wear profile. The result is consistent with the general observation that frictional contact and support compliance must be represented when local wear distribution is of interest [4], [13].

2. Running-In and Wear Evolution

For the normal-only case, the source report describes pressure redistribution over approximately 1900 revolutions. The initial central pressure peak of about 0.8 MPa decreases toward approximately 0.4 MPa as the most heavily loaded nodes wear and neighbouring regions progressively carry more load. The corresponding maximum wear depth is reported as approximately 4.5 μm. This represents a self-limiting running-in process in the simplified case without tangential traction.

When tangential friction is included, the reported running-in process extends to approximately 2900 revolutions, corresponding to about 2500 m of sliding at an effective radius of 0.137 m.

The final pressure is described as approximately 0.2–0.4 MPa over the stabilised region. The combined-friction wear profile is asymmetric and reaches approximately 15 μm maximum depth. The greater wear relative to the normal-only case is attributed to the non-uniform pressure field produced by frictional tipping.

The reported values should be interpreted within the assumptions of the model. In particular, the 4.5 μm and 15 μm results correspond to different loading representations and are not directly interchangeable measures of a single operating cycle.

© 2026 IJSRET

3. Comparative Material Performance

Table 2. Comparative Results Reported for the Three Lining Materials

Material	Initial peak p (MPa)	Steady p (MPa)	Max wear (μm)	Running-in (rev.)
Organic composite	1.20	0.68	15.0	2400
Semi-metallic	1.65	0.74	6.2	4100
Ceramic matrix	2.10	0.82	2.1	5800

The initial peak pressure rises with lining stiffness: 1.20 MPa for organic, 1.65 MPa for semi-metallic, and 2.10 MPa for ceramic. The steady-state pressure values reported after running-in are 0.68, 0.74, and 0.82 MPa, respectively. The maximum wear depth decreases from 15.0 μm for the organic lining to 6.2 μm for the semi-metallic lining and 2.1 μm for the ceramic candidate. Thus, the semi-metallic and ceramic results correspond to approximately 41% and 14% of the organic baseline wear depth.

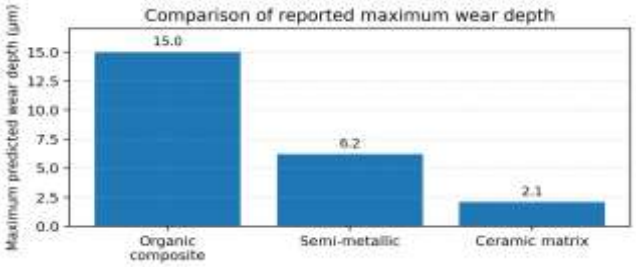


Fig. 1. Reported maximum wear depth for the three friction-lining candidates.

The running-in duration increases from 2400 revolutions for the organic candidate to 4100 for semi-metallic and 5800 for ceramic. The reported trend is consistent with the combined influence of a lower wear coefficient and greater stiffness: the more wear-resistant material removes less material per revolution and requires a longer sliding distance to redistribute the initial pressure concentration. The organic lining adapts more quickly but experiences the greatest material loss. The ceramic lining provides the lowest predicted wear but has the highest initial and steady-state pressure values and the longest running-in period. The semi-metallic candidate offers an intermediate response.

These comparisons are useful for screening, but they do not establish an overall best material. A complete brake-pad selection must also consider friction stability, fade resistance, thermal conductivity, noise and vibration, rotor compatibility, cost, manufacturability, and environmental performance [2], [7].

4. Interpretation and Engineering Implications

The numerical trends suggest three practical implications. First, the pressure field should be evaluated with tangential traction when the objective is to predict local wear asymmetry. Second, progressive geometry updates are important because wear changes the contact state and can reduce local pressure peaks during running-in. Third, a material with the lowest wear coefficient may not produce the most uniform initial pressure or the shortest running-in period. Material selection should therefore be treated as a multi-criteria engineering decision rather than a simple minimum-wear problem.

VI. MODEL LIMITATIONS AND VALIDATION REQUIREMENTS

Several limitations must be considered before the reported values are used for design decisions. The analysis is described as isothermal and does not fully couple frictional heat generation, transient temperature, thermal expansion, and temperature-dependent material properties. The wear coefficient is treated as an empirical constant, although real friction materials may exhibit dependence on temperature, pressure, speed, humidity, and third-body layer formation. Some surrounding brake components are simplified or treated as rigid, which may affect caliper compliance and the predicted pressure field.

The source report does not provide, in the material extracted for this paper, a complete set of geometry dimensions, mesh-convergence data, solver tolerances, uncertainty bounds, or independent experimental measurements for every material case. Therefore, the results in Tables I and II are reproduced as reported project outputs and are not claimed as independently verified results of the present paper. Before publication or submission, the model should be rerun with archived CAD and solver files, mesh-independence should be demonstrated, and predicted wear should be compared with pin-on-disc or brake-dynamometer measurements under matching conditions.

A useful validation protocol is to compare contact-pressure distribution, pad displacement, temperature (if thermal analysis is performed), and measured wear depth. Percentage deviation may be calculated as:

$$\text{Error (\%)} = |X_{FE} - X_{ref}| / |X_{ref}| \times 100 \qquad (5)$$

© 2026 IJSRET

where X_FE is the finite-element prediction and X_ref is the corresponding experimental or published reference value. The comparison is meaningful only when the geometry, units, material formulation, and operating conditions are sufficiently similar.

VII. CONCLUSION

This paper has presented an IEEE-style synthesis of a three-dimensional finite-element and Archard-wear framework for automotive disc-brake friction linings. The supplied project report describes a 2.5 kN normal actuation load, frictional pad–rotor contact, rigid rotor and piston representations, and an iterative APDL wear update. The reported results show that adding tangential friction changes the contact-pressure field from a near-symmetric distribution to an asymmetric leading-edge concentration, which in turn produces non-uniform wear. For the normal-only case, the report gives approximately 4.5 μm maximum wear after about 1900 revolutions. For the combined sliding-friction case, it reports approximately 15 μm maximum wear after about 2900 revolutions (approximately 2.5 km sliding distance). In the material comparison, maximum wear depths are 15.0 μm, 6.2 μm, and 2.1 μm for organic, semi-metallic, and ceramic candidates, respectively. The organic lining exhibits the shortest running-in period, whereas the ceramic candidate provides the lowest predicted wear but requires the longest running-in period and has the highest contact-pressure values. The semi-metallic lining presents an intermediate balance.

The findings support the use of contact-pressure-informed wear modelling for comparative design studies. However, the conclusions remain bounded by the reported model assumptions and require independent reproduction and experimental validation. Future work should incorporate fully coupled thermo-mechanical analysis, temperature- and velocity-dependent wear coefficients, flexible caliper behaviour, uncertainty quantification, and optimisation of pad geometry for more uniform contact.

Acknowledgment
The author gratefully acknowledges the guidance of Dr. T. Y. Badgujar and the support of the Department of Mechanical Engineering, Late G N Sapkal College of Engineering, Anjneri, Nashik.

REFERENCES

1. Z. Tang, H. Yin, J. Zhao, and C. Ding, “Coupled wear-thermal-structural multiphysics field analysis of friction linings in disk brakes,” Proc. IMechE, Part D: J. Automobile Engineering, vol. 239, no. 23, pp. 9765–9779, 2025, doi: 10.1177/09544062251376102.
2. Ș. Voloacă, A. Badea-Romero, F. Badea-Romero, and M. F. Toma, “Motor vehicle brake pad wear—A review,” Vehicles, vol. 7, no. 2, Art. no. 52, 2025, doi: 10.3390/vehicles7020052.
3. G. S. Gurumoorthy, S. Grandhi, and S. S. Sridhar, “Brake pad wear prediction using finite element techniques,” SAE Technical Paper 2021-01-0810, Apr. 2021, doi: 10.4271/2021-01-0810.
4. G. Riva, F. Varriale, and J. Wahlström, “A finite element analysis (FEA) approach to simulate the coefficient of friction of a brake system starting from material friction characterization,” Friction, vol. 9, pp. 191–200, 2021, doi: 10.1007/s40544-020-0397-9.
5. D. Li, D. Sun, H. Xi, and J. Dai, “Review on the mechanism of failure mode based on mechanical performance analysis of brake disc,” Advances in Mechanical Engineering, vol. 16, no. 12, 2024, doi: 10.1177/16878132241298368.
6. Z. Sha, Q. Hao, J. Yin, F. Ma, Y. Liu, and S. Zhang, “Wear calculation and life prediction model of disc brake based on elastoplastic contact mechanics,” Advances in Mechanical Engineering, 2022, doi: 10.1177/16878132221093136.
7. P. Grześ et al., “Initial selection of disc brake pads material based on the temperature mode,” Materials, vol. 13, no. 4, Art. no. 873, 2020.
8. G. Riva, J. Wahlström, and A. Alemani, “An FEA approach to simulate disc brake wear and airborne particle emissions,” Tribology International, vol. 138, pp. 90–98, 2019.
9. Z. Zhang et al., “Simulation study on friction and wear law of brake pad in high-power disc brake,” Mathematical Problems in Engineering, vol. 2019, Art. no. 6250694, 2019, doi: 10.1155/2019/6250694.
10. B.-C. Goo, “A study on the contact pressure and thermo-elastic behavior of a brake disc-pad by infrared images and finite element analysis,” Applied Sciences, vol. 8, no. 9, Art. no. 1639, 2018, doi: 10.3390/app8091639.
11. M. J. Han, C. H. Lee, T. W. Park, J. M. Park, and S. M. Son, “Coupled thermo-mechanical analysis and shape optimization for reducing uneven wear of brake pads,” International Journal of Automotive Technology, vol. 18, pp. 1027–1035, 2017, doi: 10.1007/s12239-017-0100-y.
12. N. Strömberg, “A virtual test rig for disc brake systems by adopting a thermo-flexible multi-body approach,” SAE Technical Paper 2016-01-1932, 2016, doi: 10.4271/2016-01-1932.

© 2026 IJSRET

13. A. R. Abu Bakar and H. Ouyang, “Prediction of disc brake contact pressure distributions by finite element analysis,” Jurnal Teknologi, vol. 43, 2012, doi: 10.11113/jt.v43.755.
14. J. F. Archard, “Contact and rubbing of flat surfaces,” Journal of Applied Physics, vol. 24, no. 8, pp. 981–988, 1953.
15. H. Ouyang, A. R. Abu-Bakar, and L. Li, “A combined analysis of heat conduction, contact pressure and transient vibration of a disk brake,” International Journal of Vehicle Design, vol. 51, nos. 1–2, pp. 190–206, 2009, doi: 10.1504/IJVD.2009.027121.
16. H.-J. Cho and C.-D. Cho, “A study of thermal and mechanical behaviour for the optimal design of automotive disc brakes,” Proc. IMechE, Part D: J. Automobile Engineering, vol. 222, no. 6, pp. 895–915, 2008, doi: 10.1243/09544070JAUTO722.

© 2026 IJSRET